A novel 2-RC equivalent model based on the self-discharge effect for accurate state-of-charge estimation of lithium-ion batteries.

WANG, S., CAO, J., XIE, Y., GAO, H. and FERNANDEZ, C.

2022

Int. J. Electrochem. Sci., 17 **(2022)** Article Number: 22072, doi: 10.20964/2022.07.60

International Journal of
ELECTROCHEMICAL
SCIENCE
www.electrochemsci.org

A Novel 2-RC Equivalent Model Based on the Self-Discharge Effect for Accurate State-Of-Charge Estimation Of Lithium-Ion Batteries

Shunli Wang[1,*], *Jie Cao*[1], *Yanxin Xie*[1], *Haiying Gao*[1], *Carlos Fernandez*[2]

[1] School of Information Engineering, Southwest University of Science and Technology, Mianyang 621010, China
[2] School of Pharmacy and Life Sciences, Robert Gordon University, Aberdeen, UK
[*]E-mail: 497420789@qq.com.

Received: 2 December 2021 / *Accepted:* 5 May 2022 / *Published:* 6 June 2022

Accurate lithium-ion battery state-of-charge estimation and effective equivalent modeling are important for real-time status monitoring and safety control of lithium-ion batteries. To solve the problem of low accuracy of the second-order RC equivalent model, based on a large number of experimental analyses on the ternary lithium-ion battery, the traditional second-order RC equivalent model was improved, and the self-discharge effect was incorporated into the equivalent model establishment. By measuring the change of the open-circuit voltage of the lithium-ion battery within 30 days in the resting state, the identification of the characteristic parameters of the self-discharge circuit is completed. The experimental results show that, compared with the traditional second-order RC equivalent model, the Self-Discharge-2-RC(SD-2-RC) equivalent model can better simulate the working state of the lithium-ion battery. The maximum error between the analog voltage and the real voltage is less than 0.03V, and its accuracy can be up to 99.3% or more. Based on the accurate establishment of the equivalent model, the Adaptive Extended Kalman filter algorithm is used to estimate the SOC. The algorithm has a fast convergence speed and a good tracking effect. The estimation accuracy can reach more than 96%, and the accurate estimation of the state of charge is realized. This research provides a theoretical basis for the establishment of a more accurate lithium-ion battery equivalent circuit model.

Keywords: Self-discharge effect; Self-Discharge-2-RC equivalent model; Adaptive Extended Kalman Filter

1. INTRODUCTION

In recent years, due to the exhaustion of fossil energy and the increasingly serious environmental pollution problems[1], new energy has become the main direction of China's current energy development[2]. With the rapid development of new energy vehicles, its complete vehicle and drive

technologies have matured day by day[3]. As one of the three-electric systems of new energy vehicles, power batteries still have a lot of room for improvement in related technologies, such as low battery usage[4], Problems such as short cycle life are still bottlenecks in the development of core technologies for new energy vehicles[5]. Lithium-ion batteries have the advantages of high energy density and large output power and have an important position in the field of renewable energy[6]. With the increasing application of lithium-ion batteries in the new energy automobile industry, the health of lithium-ion batteries has received more and more attention[7]. Scientific lithium-ion battery controls strategy and accurate lithium-ion battery health status[8] detection play a vital role in the full display of lithium-ion battery performance and safety control[9]. Establishing an accurate battery model can more intuitively describe the influencing factors and operating characteristics of the state of charge of the lithium-ion battery[10], and it is also the key to improving the accuracy of the lithium-ion battery SOC estimation[11], which is of great significance for the accurate estimation of the lithium-ion battery SOC.

At present, the commonly used equivalent circuit models include the internal resistance model, Thevenin model, and second-order RC model[12]. The internal resistance model has few parameters and is easy to identify, but the fixed-value resistance is used to characterize the ohmic internal resistance and polarization internal resistance when the battery is working[13], ignoring the influence of polarization effects, temperature and other factors on internal resistance, which is only suitable for accuracy The less demanding situation[14]. The Thevenin model considers the polarization effect of the battery based on the internal resistance model, which can more accurately simulate the charging and discharging behavior of the battery and characterize the dynamic and static characteristics of the battery, but there are still shortcomings in the face of higher model accuracy requirements[15]. The second-order RC model uses two RC network structures to characterize the concentration polarization and electrochemical polarization of the lithium-ion battery, which can reflect the dynamic and static characteristics of the lithium-ion battery, and the model has good real-time solution and the parameters are easy to identify. According to the challenging working environment of aviation lithium-ion battery, Wang et al.[16] proposed a splicing equivalent circuit model according to the expression of special conditions of aviation lithium-ion battery, which realized the precise working conditions and working process of lithium-ion-ion battery pack. Mathematical expression. Ji et al.[17] proposed a varistor-capacitor second-order RC equivalent circuit model, and analyzed and verified the effect of fixed resistance and variable capacitance on the estimation accuracy in the equivalent circuit model. Cai et al.[18] established an equivalent circuit model with thermal characteristics based on the second-order RC model based on the thermal effect of lithium-ion batteries. The maximum error of the thermal model are within 5%. Chen et al.[19] proposed a lithium-ion battery hybrid equivalent circuit model for the problem of the low accuracy of Thevenin model. The state of charge was added to the model to improve performance, which can more accurately reflect the polarization effect of the lithium-ion battery.

The above-mentioned research has become more and more accurate for the equivalent modeling of lithium-ion batteries, but ignores the influence of the self-discharge effect of the lithium-ion battery itself on the open circuit voltage. This paper improves on the problems of the traditional second-order RC model and proposes the SD-2-RC equivalent model, which incorporates the self-discharge process of the lithium-ion battery into the establishment of the equivalent circuit model, through the self-discharge resistance Ra and self-discharge The RC loop composed of capacitor C_b characterizes the self-

discharge process in detail. Perform (Hybrid Pulse Power Characterization, HPPC) experiments and open-circuit voltage measurement experiments[20] at a constant temperature, and obtain a large amount of experimental data. The characteristic parameters of resistance, self-discharge resistance, self-discharge capacitor, and two RC loops were identified, and the SD-2-RC equivalent model simulation of lithium-ion battery was built using MATLAB/Simulink to verify and analyze the identification results of various characteristic parameters. It provides an experimental and theoretical basis for the subsequent development of accurate estimation of the SOC and Battery Management System (BMS) of lithium-ion batteries.

2. THEORETICAL ANALYSIS

2.1 SD-2-RC equivalent circuit model

Due to the multi-parameter coupling process of lithium-ion batteries, it is a highly complex nonlinear electrochemical energy storage device[21]. On the one hand, it is difficult to use accurate formulas to characterize the complex electrochemical reactions, energy transfer, and charge of lithium-ion batteries during operation. Mobile, etc., are difficult to be applied in actual engineering[22]; on the other hand, completely using experimental data to simulate the working process of lithium-ion batteries (such as neural networks) requires a lot of data input and learning[23], so the hybrid modeling method is usually more common[24]. Currently, electrochemical models, coupling models, thermodynamic models and equivalent circuit models are widely used[25]. In contrast, the equivalent circuit model does not require an in-depth analysis of the chemical reactions inside the lithium-ion battery[26]. The open-circuit voltage and polarization effect of the lithium-ion battery are described through the circuit to achieve effective characterization of the operating characteristics of the lithium-ion battery. By studying the working principles and characteristics of lithium-ion batteries, summarizing the advantages and disadvantages of the current equivalent circuit model, improving the traditional second-order RC equivalent model, and constructing the SD-2-RC equivalent circuit model for more accurate characterization for the working condition of the lithium-ion battery. The SD-2-RC model is shown in Fig. 1.

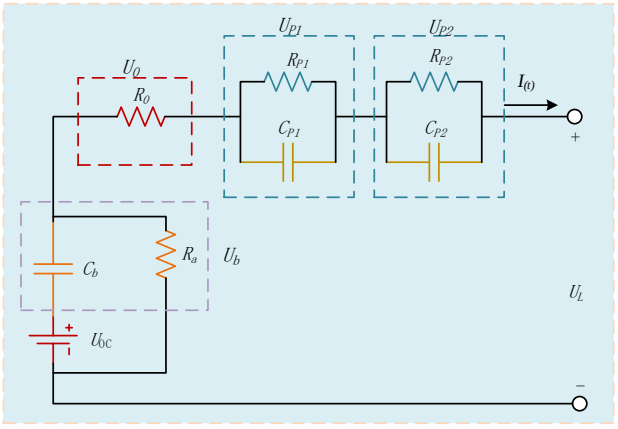

Figure 1. SD-2-RC open-circuit model

Fig. 1 is the SD-2-RC model, U_{OC} is the open circuit voltage of the lithium-ion battery; U_L is the terminal voltage of the lithium-ion battery; R_0 is the ohmic internal resistance of the lithium-ion battery, which is used to characterize the instantaneous voltage drop of the lithium-ion battery. The two loops composed of R_{P1}, C_{P1}, and R_{P2}, C_{P2} are used to characterize the polarization effect during the charging and discharging process of the lithium-ion battery; $I(t)$ are the circuit loop current, and the discharge direction is positive. In order to better reflect the self-discharge effect when the lithium-ion battery is not connected to a load, the model adds C_b and R_a on the original basis to characterize the self-discharge process of the lithium-ion battery when the lithium-ion battery is left unconnected for a long time. By analyzing the circuit structure of the equivalent model, according to Kirchhoff voltage law, the voltage relationship in the circuit is shown in equation (1).

$$\begin{cases} U_L = U_{oc} - U_b - U_0 - U_{p1} - U_{p2} \\ i_L = C_{p1}\dfrac{dU_{p1}}{dt} + \dfrac{U_{p1}}{R_{p1}} = C_{p2}\dfrac{dU_{p2}}{dt} + \dfrac{U_{p2}}{R_{p2}} \end{cases} \tag{1}$$

Set SOC_0 as the initial value of the state, combined with the definition of SOC, the SOC value at time k in the continuous state can be obtained, as shown in equation (2).

$$SOC_k = SOC_0 - \frac{\eta \int_0^k i(t)dt}{Q_0} \tag{2}$$

In the formula (2), η is the discharge efficiency of the lithium-ion battery, and η=1 in a room temperature environment. Q_0 is the rated capacity of the lithium-ion battery. Discretize the equivalent circuit model[27], and the discretization formula is shown in equation (3).

$$SOC_k = SOC_0 - \frac{\eta \Delta t}{Q_0} i_k \tag{3}$$

Through SOC definition formula (2), choosing $x_k = \left[SOC_k, U_{p1,k}, U_{p2,k}, U_b\right]^T$ as the state space variable, i_k as the input variable, and $y_k = \left[U_{L,k}\right]$ as the output variable, the discrete space state equation of the model can be obtained. As shown in equation (4).

$$\begin{cases} x_{k+1} = \begin{bmatrix} 1 & 0 & 0 & 0 \\ 0 & e^{-\frac{\Delta t}{\tau_1}} & 0 & 0 \\ 0 & 0 & e^{-\frac{\Delta t}{\tau_2}} & 0 \\ 0 & 0 & 0 & 1 \end{bmatrix} x_k + \begin{bmatrix} -\dfrac{\Delta t}{Q_N} \\ R_1\left(1 - e^{-\frac{\Delta t}{\tau_1}}\right) \\ R_2\left(1 - e^{-\frac{\Delta t}{\tau_2}}\right) \\ \dfrac{1}{C_b} \end{bmatrix} i_k + w_k \\ y_k = U_{oc,k} - R_0 i_k + \begin{bmatrix} 0 \\ -1 \\ -1 \\ -1 \end{bmatrix} x_k + v_k \end{cases} \tag{4}$$

In formula (4), Δt is the discrete sampling interval; $\tau_1 = R_{p1}C_{p1}$, $\tau_2 = R_{p2}C_{p2}$; $w_k$is the system noise at time k; and v_k is the measurement error at time k.

2.2 Test method selection and parameter identification

After determining the lithium-ion battery equivalent model, since the parameters of the various electronic components in the model cannot be directly measured by the instrument, it is necessary to adopt corresponding experimental methods for parameter identification. The Hybrid Pulse Power Characterization is an experimental procedure for determining the dynamic power capability of lithium-ion batteries using prescribed test methods. A pulse test is set at every interval of 0.1 in the SOC value, and the parameters are identified by analyzing the working characteristics of the lithium-ion battery. Fig. 2 shows the pulse voltage curve when SOC=0.6.

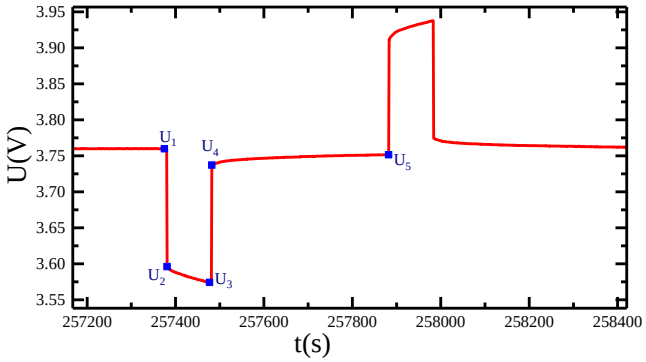

Figure 2. One HPPC cycle

From the experimental curve, it can be seen that the moment U_1 in Fig. 2 is the moment when the lithium-ion battery discharge starts, and the existence of the ohmic internal resistance R_0 of the lithium-ion battery causes the voltage of U_1~U_2 to sag and the voltage of U_3 to U_4 to rise[28]. Therefore, the ohmic internal resistance R_0 can be directly solved by the voltage change in this section. As shown in equation (5).

$$R_0 = \frac{|U_1 - U_2| + |U_3 - U_4|}{2I} \tag{5}$$

After several HPPC tests on the 4.2V/40A ternary power lithium-ion battery, it is found that if there is an error during the test, it will greatly affect the test data and the result of parameter identification. In order to reduce the influence of errors on the parameter identification results, more accurate parameter values can be obtained. In this research, on the basis of the HPPC test, the pulse charging experiment and the pulse discharging experiment were innovatively carried out.

In the pulse charging experiment, a 20A constant current was used to discharge the lithium-ion battery. After reaching the cut-off voltage of 2.75V, a charging pulse was set at an interval of 0.1 SOC value until the charging was completed. Fig. 3 is a flow chart of the pulse charging test.

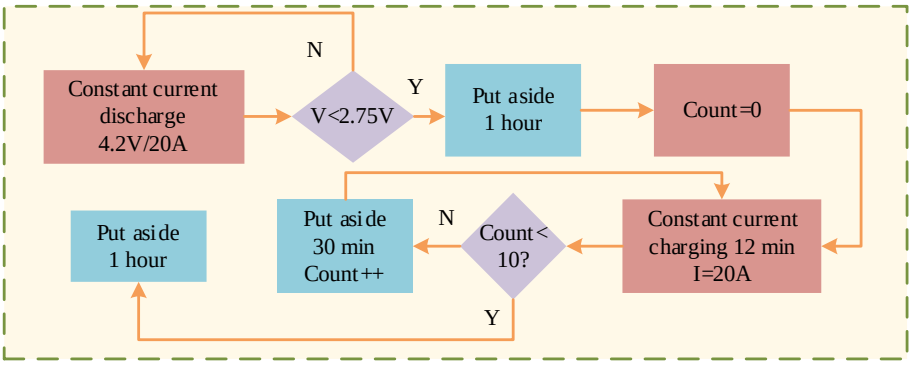

Figure 3. Pulse charging test flow chart

In the pulse discharge experiment, use a constant current of 20A to charge the lithium-ion battery. When the charging current I<2A (0.05C), the lithium-ion battery can be considered to have been charged. Set a discharge pulse every interval of 0.1 SOC value until the discharge is complete. Fig. 4 is a flow chart of the pulse discharge test.

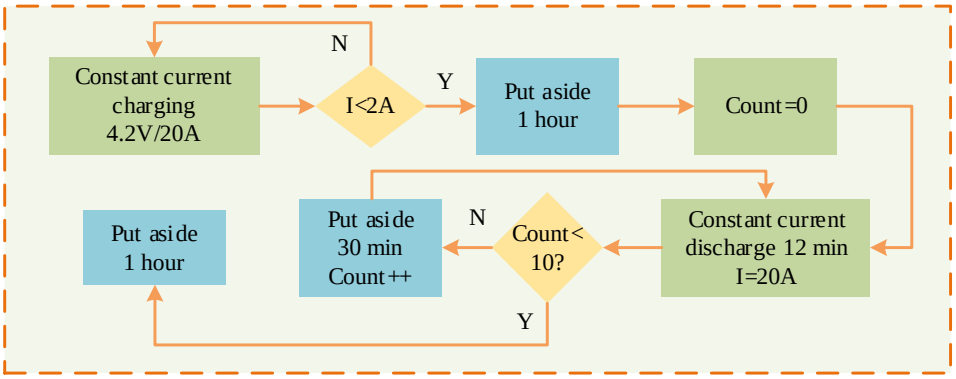

Figure 4. Pulse discharging test flow chart

After performing the above two sets of tests many times, the two sets of data with the smallest deviation were selected for plotting in Origin. Fig. 5 is a graph of the pulse charging test. A total of 10 pulse charging cycles were performed during the pulse discharge test. Fig. 6 is a graph of the pulse discharge test. A total of 10 pulse discharge cycles were performed. Since the voltage data at the cut-off voltage is not referenced, it is omitted.

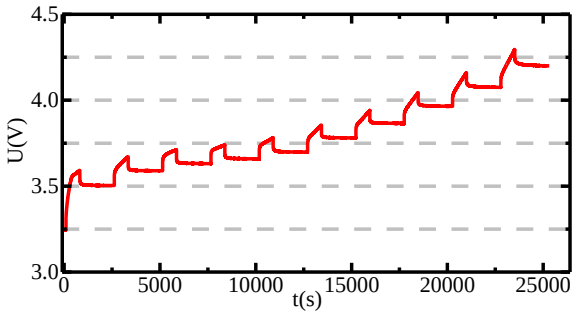

Figure 5. Pulse charging experiment curve

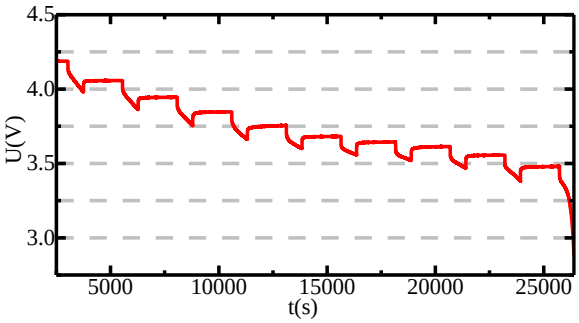

Figure 6. Pulse discharge experiment curve

In Fig. 2, the slow drop of U_2~U_3 segment voltage during discharge is due to the existence of the internal polarization effect of the lithium-ion battery, which is equivalent to the zero-state response of the RC loop in the circuit[29]; the slow voltage of U_4~U_5 segment after the discharge is over the rise is also due to the existence of the internal polarization effect of the lithium-ion battery, which is equivalent to the zero input response of the RC loop in the circuit[30]. Select the data during U_2~U_3, according to the terminal voltage expression of the lithium-ion battery, the corresponding characteristic parameters can be calculated. When curve fitting the lithium-ion battery voltage rebound curve, it is necessary to determine the fitting equation. Therefore, it is necessary to calculate the circuit equation of the SD-2-RC model and analyze[31] the SD-2-RC equivalent circuit model. When the battery is in a discharging state, the terminal voltage U of the battery is equal to the open-circuit voltage U_{OC} minus the sum of the partial pressure of the self-discharge circuit, the ohmic internal resistance R_0, and the partial pressure of the two RC circuits:

$$U = U_{OC} - U_b - U_0 - U_{P1} - U_{P2} \tag{6}$$

In equation (6), U_0 is the partial voltage of the ohmic internal resistance R_0; U_b represents the voltage division of the self-discharge effect; U_{P1} represents the voltage division of the parallel circuit of R_{P1} and C_{P1}; U_{P2} represents R_{P2}, C_{P2} The partial pressure of the parallel circuit.

During the lithium-ion battery charging and discharging experiment, when the battery is suddenly left standing, the current i in the loop suddenly becomes 0. At this time, the self-discharge loop part is equivalent to an open circuit, and the two RC parallel loops have zero input response. The first-order transient response analysis can be obtained:

$$U_{P1}(t) = i(t)R_{P1}e^{-\frac{t}{R_{P1}C_{P1}}} \quad (7)$$

$$U_{P2}(t) = i(t)R_{P2}e^{-\frac{t}{R_{P2}C_{P2}}} \quad (8)$$

Through the above formula, a continuous battery model equation can be established, as shown in equation (9):

$$U = U_{OC} - i(t)R_{P1}e^{-\frac{t}{\tau_1}} - i(t)R_{P2}e^{-\frac{t}{\tau_2}} \quad (9)$$

In formula (9), τ_1 and τ_2 are the time constants of the two RC parallel loops in the equivalent model circuit, respectively, $\tau_1 = R_{P1}C_{P1}$, $\tau_2 = R_{P2}C_{P2}$. In order to simplify the identification of equivalent model parameters, you can use the Curve Fitting tool in MATLAB to perform custom parameter fitting. The custom fitting equation is shown in equation (10):

$$U = f - ae^{-ct} - be^{-dt} \quad (10)$$

In the SD-2-RC model, the self-discharge loop effectively characterizes the self-discharge effect of the lithium-ion battery. In order to accurately characterize the self-discharge effect, it is necessary to identify the self-discharge resistance R_a and the self-discharge capacitor C_b in the self-discharge loop. C_b characterizes the voltage change caused by the current accumulation effect in the lithium-ion battery, and the value of C_b can be calculated from the voltage change from U_1 to U_5, as shown in equation (11).

$$U_1 - U_5 = \frac{1}{C_b}\int Idt \quad (11)$$

In order to measure the self-discharge resistance R_a, the lithium-ion battery needs to be fully charged first. When the load is not connected, the lithium-ion battery is placed in a thermostat for 30 days, and the change trend of its open circuit voltage is recorded. The relationship between voltage and current in the resting state is shown in equation (12).

$$U_b = \Delta U_{oc} = U_{oc0}\left(1 - e^{-\frac{t}{R_aC_b}}\right) \quad (12)$$

After testing, the initial open circuit voltage U_{oc0} of the lithium-ion battery is 4.1869V. After being left in a constant temperature environment for 30 days, the open circuit voltage U_{oc} drops to 4.1718V. Take t=60×60×24×30=2592000s, on this basis, R_a can be calculated according to equation (13).

$$R_a = \frac{-t}{C_b \times Ln\left(1 - \frac{\Delta U_{oc}}{U_{oc0}}\right)} \quad (13)$$

2.3 Adaptive extended Kalman filter algorithm

Extended Kalman Filter, as the optimal linear estimation method, is a prediction-correction method that can predict the data at the next moment and give the optimal solution[32]. Under ideal circumstances, the system noise is usually considered to be zero mean white noise. In this case, the Kalman filter algorithm usually has a better effect on the estimation of the SOC of the lithium-ion battery. However, since zero-mean white noise does not exist in practical engineering applications, this assumption is not true[33]. In the actual working process of the lithium-ion battery system, unknown noises are often collected and interfered with, which may cause the collected data to exceed its normal

range. In response to this problem, the use of the Adaptive Extended Kalman filter algorithm can greatly reduce the impact of SOC estimation caused by system noise[34].

(1) State initialization:

$$\hat{x}_0 = E[x_0] \tag{14}$$

$$P_0 = E[(x_0 - \hat{x}_0)(x_0 - \hat{x}_0)^T] \tag{15}$$

x_0 is the initial state estimation value of the system, and P_0 is the initial error covariance matrix of the system.

(2) Status update:

$$\hat{x}_{k+1} = A_k\hat{x}_k + B_k u_k + \Gamma q_k \tag{16}$$

$$P_{k+1} = A_k P_k A_k^T + \Gamma Q_k \Gamma^T \tag{17}$$

Estimate the state value $\hat{x}_{k+1}$ at the next moment through the state value $\hat{x}_k$ at the current moment, and update the error covariance matrix P_{k+1}.

(3) Calculate the Kalman gain matrix:

$$K_k = P_{k+1}C^T(CP_{k+1}C^T + P_k)^{-1} \tag{18}$$

(4) State estimation:

$$\hat{x}_{k+1} = \hat{x}_k + [y_k - (C\hat{x}_k + Du_k + d - r_k)] \tag{19}$$

$$P_{k+1} = (E - K_{k+1}C_{k+1})P_k \tag{20}$$

The adaptive Kalman filter measures and updates the error covariance matrix and the state through the state measurement value at the current moment, and obtains a more accurate estimation result at the next moment. E is the identity matrix, and the state estimate at time $k+1$ is equal to the sum of the state a priori estimate at time k and the weighted correction value. The new information obtained through the measurement makes the uncertainty of the state continue to decrease, that is, P_k continues to decrease[35].

(5) Noise update:

$$q_{k+1} = (1 - d_k)q_k + d_k G(\hat{x}_{k+1} - A\hat{x}_{k+1} - Bu_k) \tag{21}$$

$$Q_{k+1} = (1 - d_{1-k})Q_k + d_k G\left(L_{k+1}\tilde{y}_{k+1}\tilde{y}_{k+1}^T\tilde{L}_{k+1}^T + P_k - AP_{k+1|k}A^T\right)G^T \tag{22}$$

$$r_{k+1} = (1 - d_{1-k})r_k + d_k\left(y_{+1} - C\hat{x}_{k+1|k} - Du_k - d\right) \tag{23}$$

$$R_{k+1} = (1 - d_{1-k})R_k + d_k\left(\tilde{y}_{k+1}\tilde{y}_{k+1}^T - CP_{k+1|k}C^T\right) \tag{24}$$

Among them, $G = (\Gamma^T\Gamma)^T$, Γ is the noise driving matrix, $d_k = \frac{1-b}{1-b^{k+1}}$; b is the forgetting factor, $0<b<1$. The function of the forgetting factor is that when b is larger, the system forgets slowly and pays more attention to data at historical moments; when b is smaller, the system forgets faster and pays more attention to current data[36]. Through real-time estimation and update of noise q_{k+1}、Q_{k+1}、r_{k+1}、R_{k+1}, the continuous correction of SOC is realized and the goal of adaptive filter is achieved[37], Fig. 7 is a flow chart of the AEKF algorithm for SOC estimation.

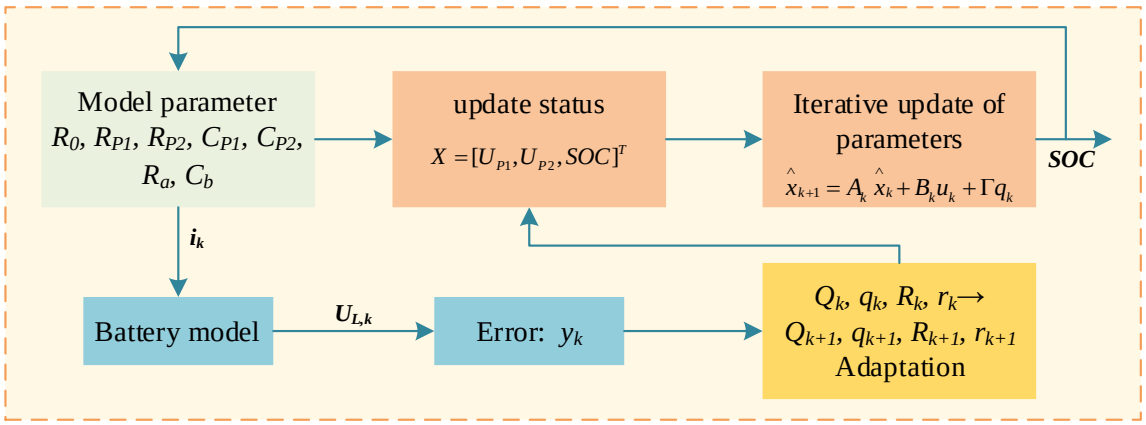

Figure 7. SOC estimation method based on AEKF

3. ANALYSIS OF RESULTS

3.1 Identification of ohmic resistance and polarization resistance and capacitance

Using the offline parameter identification method, through the calculation process of the characteristic parameters such as ohmic resistance R_0, polarization capacitance C_{p1}、C_{p2} and polarization resistance R_{p1}、R_{p2} derived in 1.2, the model characteristic parameters under pulse charging experiment and pulse discharge experiment are obtained respectively parameters, find the average value of the parameters at the corresponding SOC point, this method can correspondingly improve the accuracy of the equivalent model parameter identification[38]. The identification results of the characteristic parameters in the SD-2-RC model can be obtained at the equidistant points from SOC=1 to SOC=0.1, as shown in Tab. 1.

Table 1. Model parameter identification results under different SOC states

SOC/100%	U_{OC}/V	R_0/mΩ	R_1/mΩ	R_2/mΩ	C_1/F	C_2/F	C_b/kF
1	4.1834	3.782391	0.23415	0.096668	75110.09249	11688.90429	16650.625
0.9	4.0550	3.801159	0.264755	0.14494	104715.2591	13124.27287	20319.40678
0.8	3.9446	3.743603	0.255746	0.136732	77153.2597	13491.23427	18443.76923
0.7	3.8467	3.723006	0.278725	0.13028	68560.38241	10718.84289	16653.20833
0.6	3.7565	3.731091	0.258249	0.106352	66624.88596	11977.96928	14271.96429
0.5	3.6814	3.745525	0.23529	0.0778128	70905.47942	14896.6622	26065.8913
0.4	3.6449	3.762955	0.221484	0.0955818	92596.39501	19281.68342	25503.38298
0.3	3.6154	3.758035	0.240544	0.104735	107980.2453	16848.32457	26065.8913
0.2	3.5577	3.795565	0.252454	0.0985796	63940.59598	8376.619566	20322.55932
0.1	3.4818	3.903757	0.30079	0.190183	51760.61072	4385.397919	16885.14085

3.2 Identification of characteristic parameters of self-discharge circuit

In the SD-2-RC model, the self-discharge loop effectively characterizes the self-discharge effect. In order to accurately characterize the self-discharge effect, it is necessary to identify the self-discharge

resistance R_a and the self-discharge capacitor C_b in the loop. C_b characterizes the voltage change caused by the current accumulation effect, and the value of C_b can be calculated from the voltage change from U_1 to U_5, as shown in equation (25). Where I is the current in the discharge phase.

$$U_1 - U_5 = \frac{1}{C_b}\int Idt \tag{25}$$

To accurately measure the self-discharge resistance R_a, the lithium-ion battery needs to be fully charged first. When the load is not connected, place the lithium-ion battery in a thermostat and set the ambient temperature to be constant. Leave it for 30 days and record its open circuit voltage. The trend of change. According to KVL, the relationship between voltage and current in the shelving state can be calculated[39], as shown in equation (26).

$$U_b = \Delta U_{oc} = U_{oc0}\left(1 - e^{-\frac{t}{R_a C_b}}\right) \tag{26}$$

After testing, the initial open circuit voltage U_{oc0} of the lithium-ion battery was 4.1869V. After being left in a constant temperature environment for 30 days, the open circuit voltage U_{oc} dropped to 4.1618V. The data change of the open circuit voltage within 30 days can be seen from Tab. 2.

Table 2. Open circuit voltage change

Voltage/V									
Day1	4.1869	Day7	4.179	Day13	4.1725	Day19	4.1692	Day25	4.165
Day2	4.1853	Day8	4.1779	Day14	4.1719	Day20	4.1685	Day26	4.1644
Day3	4.1833	Day9	4.1768	Day15	4.1712	Day21	4.1679	Day27	4.1639
Day4	4.1821	Day10	4.1755	Day16	4.1709	Day22	4.1676	Day28	4.1633
Day5	4.1812	Day11	4.1746	Day17	4.1703	Day23	4.1671	Day29	4.1626
Day6	4.1801	Day12	4.1738	Day18	4.1699	Day24	4.1654	Day30	4.1618

Take t=60×60×24×30=2592000s. After calculation, the value of C_b can be obtained, as shown in Tab. 1. Here, the average value of C_b is taken as 20118.18394kF. On this basis, R_a can be calculated according to equation (27).

$$R_a = \frac{-t}{C_b \times Ln\left(1 - \frac{\Delta U_{oc}}{U_{oc0}}\right)} = 35.6596\Omega \tag{27}$$

4. MODEL VALIDATION ANALYSIS

To verify the feasibility of the AEKF algorithm and the SD-2-RC model for SOC estimation, based on the construction of the equivalent circuit model, the experimental data under various experimental conditions are obtained, and the AEKF algorithm is used to complete the comparison of the 2-RC model and the SD The SOC estimation simulation of the -2-RC model, by comparing the estimation results of the 2-RC model and the SD-2-RC model based on the Ah integral estimation result, verifies the validity and reliability of the AEKF algorithm and the SD-2-RC model.

4.1 Analog voltage accuracy verification

In order to verify the validity of the SD-2-RC equivalent model proposed in this paper, the model simulation built in MATLAB/Simulink is used, and the polynomial obtained through parameter identification is input into the corresponding parameter module in the model, and input into the corresponding HPPC experiment. The current data of the model; by comparing the output simulation voltage of the model with the experimental voltage, the accuracy of the model is verified, and the model is improved and optimized on this basis.

It can be seen from Fig. 8 that blue curve is the actual voltage output curve, red curve is the simulated output voltage of the SD-2-RC model, and green curve is the simulated output voltage of the second-order RC equivalent model. In the case that the parameter identification and curve fitting adopt the same fitting order, compared with the traditional second-order RC model, the output voltage of the SD-2-RC equivalent model can better match the actual voltage curve, and the error is even greater. It is small, which proves the feasibility and effectiveness of the parameter identification method.

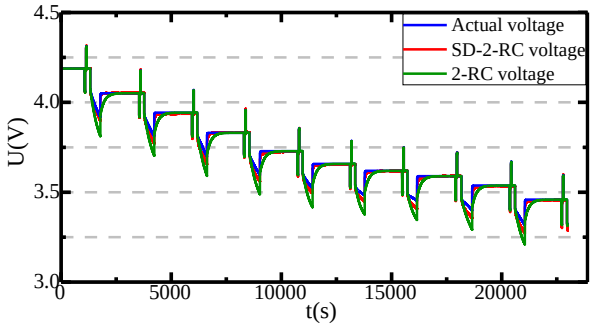

Figure 8. Comparison curve of simulated voltage and real voltage output

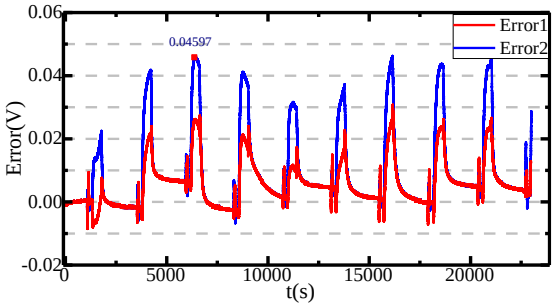

Figure 9. Voltage output error curve

Fig. 9 shows the output voltage error curve. The model did not diverge during the entire simulation process. The maximum error occurred in the pulse discharge phase. This is because the sudden current change during the discharge process leads to a rapid change in the terminal voltage. At the same time, the existence of the error proves that it is equivalent. The circuit model is not completely equivalent to the complicated electrochemical reaction inside the lithium-ion battery[40]. Among them,

Error1 is the output voltage error of the SD-2-RC model. The maximum voltage error does not exceed 0.03V. The maximum voltage of the lithium-ion battery is 4.2V, so the accuracy can reach more than 99.3%. In contrast, the maximum output voltage error Error2 of the traditional second-order RC model is 0.04597V, and the accuracy is 99%. The accuracy of the SD-2-RC model has been effectively improved on the basis of the second-order RC model. This model can more accurately characterize the working characteristics of lithium-ion batteries.

3.2 Model verification under HPPC conditions

To verify the effectiveness and practicability of the SD-2-RC equivalent circuit model for improving the accuracy of lithium-ion battery SOC estimation, the experimental data was obtained by performing HPPC experiments in a constant temperature environment, and the SOC estimation under HPPC conditions was completed. The comparison curves of the true value of SOC, the estimated value of SD-2-RC and the estimated value of 2-RC are shown in Fig 10.

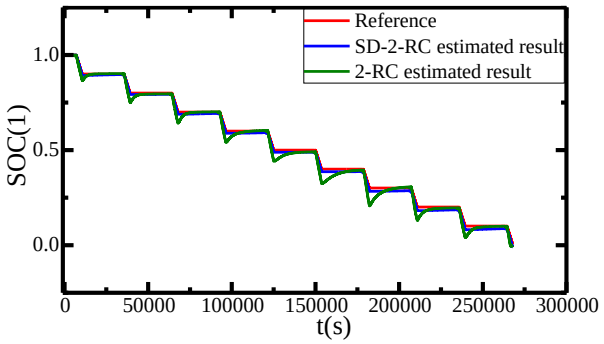

Figure 10. SOC estimation curve under HPPC conditions

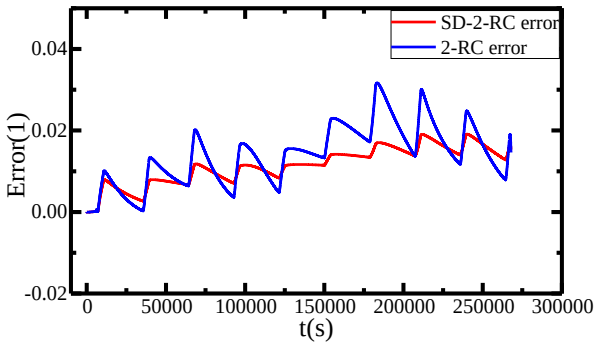

Figure 11. SOC estimation error

It can be seen from Fig. 10 that when the system noise is the same, although the traditional second-order RC model can better estimate the SOC of the lithium-ion battery, because the self-discharge effect of the battery is not considered, when the battery is discharged, due to the current sudden change, the SOC estimation curve shows a trend of first decline and then rise, and there has been a large

fluctuation. Compared with the 2-RC model, the SOC estimation curve of the SD-2-RC model has a higher degree of coincidence with the true value, which is closer to the true curve, and has greater advantages in terms of convergence speed and estimation accuracy. It can be seen from the SOC estimation error curve in Fig. 11 that on the basis of the AEKF algorithm, the SOC estimation error of the 2-RC model fluctuates greatly when the battery is discharged, and the maximum error reaches 3.16%. The SOC estimation error of the SD-2-RC model only fluctuates slightly, and the maximum error is only 1.9%. It shows that adding a self-discharge circuit on the basis of the 2-RC model can more effectively characterize the working characteristics of the lithium-ion battery, and to a certain extent can improve the estimation accuracy of the SOC.

3.3 Model verification under DST conditions

The experiment was carried out under (Dynamic Stress Test, DST) conditions, the battery was discharged at 1C, charged at 0.5C, the simulation time was 82000s, and the sampling interval was 1s to obtain the experimental data. Fig. 12 shows the overall estimated performance of the two equivalent circuit models.

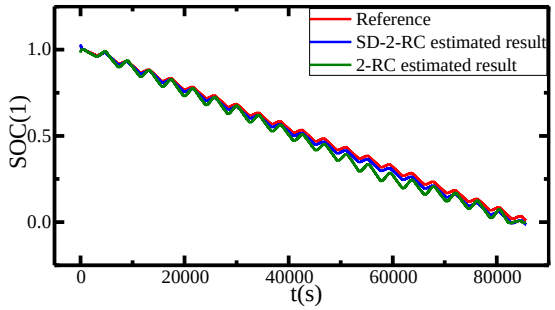

Figure 12. SOC estimation curve under DST conditions

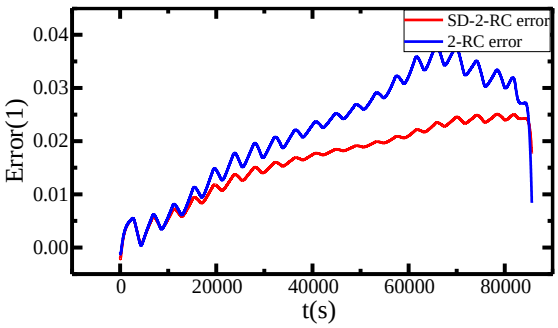

Figure 13. SOC estimation error

The two equivalent models can track the SOC value well at the initial time of estimation, but after the estimated time reaches 50000s, since the cumulative error caused by the self-discharge effect is not considered, the estimated result of the 2-RC model has a large deviation compared with the true

value. From the error curve in Fig. 13, it can be seen that the maximum error of SOC estimation is 4%. The SD-2-RC model can well realize the tracking simulation of the true value. The error fluctuation is within a reasonable range, and the SOC estimation The maximum error is 2.48%. Compared with the 2-RC model, the estimation accuracy is improved by 1.52%.

3.4 Model verification under BBDST conditions

In order to simulate and verify the influence of the SD-2-RC equivalent circuit model on SOC estimation in practical applications, this research further conducts experiments under (Beijing Bus Dynamic Stress Test, BBDST) conditions to complete a comparative analysis of the effectiveness of the two equivalent models.

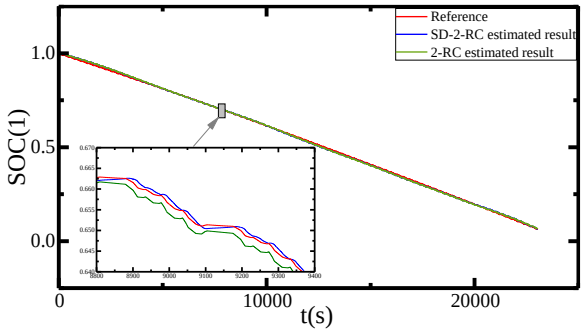

Figure 14. SOC estimation curve under BBDST conditions

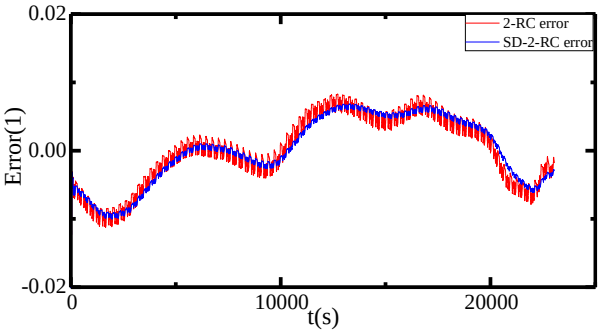

Figure 14. SOC estimation error

From the SOC estimation curve in Fig. 14, it can be seen that compared to the 2-RC model, the SOC estimation curve of the SD-2-RC model is more convergent to the true SOC value. Although the maximum estimation error of the two equivalent models is 1%, it can be seen from Fig. 15 that when the battery is charged and discharged frequently, the SOC estimation using the 2-RC model is greatly affected by the current change, and the estimation results are similar. Compared with the real value, there are larger fluctuations, and the error fluctuation of the SD-2-RC model with the self-discharge loop is

significantly reduced, and it can always be maintained within a reasonable fluctuation range. It further proves the validity and feasibility of the SD-2-RC equivalent circuit model.

5. CONCLUSION

Based on a large number of experiments on ternary lithium-ion batteries, this paper fully explores and analyzes the polarization effects and self-discharge effects of lithium-ion batteries. Based on the traditional second-order RC equivalent circuit model, the SD-2-RC equivalent circuit is established. Model. The parameter identification of the lithium-ion battery is completed through the phased charge and discharge experiment curve, and the parameter identification of the self-discharge circuit is completed by continuously recording the open circuit voltage change when the lithium-ion battery is not connected to the load. Through Simulink simulation verification, the results show that the error between the simulation voltage of the SD-2-RC model and the experimental value is not higher than 0.03V, and the simulation accuracy can reach 99.3%. In addition, on the basis of the AEKF algorithm, combined with experimental data under various working conditions for simulation analysis, the results show that the SD-2-RC equivalent model can more accurately estimate the lithium-ion battery SOC, and the estimation accuracy is above 96%. Verified the effectiveness of the SD-2-RC equivalent model, indicating that the model can provide a good model basis for lithium-ion battery modeling and simulation and SOC estimation.

ACKNOWLEDGMENTS
The work was supported by National Natural Science Foundation of China (No. 61801407).

References

1. Y. Yang, E. G. Okonkwo, G. Huang, S. Xu and Y. J. E. S. M. He, *Energy Storage Materials*, 36 (2020) 7342.
2. V. Aravindan, Y. S. Lee and S. Madhavi, *Advanced Energy Materials*, 5 (2015) 901.
3. C. Chen, R. Xiong and W. Shen, *Ieee Transactions on Power Electronics*, 33 (2018) 332.
4. E. Pomerantseva, F. Bonaccorso, X. Feng, Y. Cui and Y. J. S. Gogotsi, *Science*, 366 (2019).
5. Y. Chen, A. Dou and Y. J. F. i. M. Zhang, *Frontiers In Materials*, 8 (2021) 634667.
6. R. Fang, K. Chen, L. Yin, Z. Sun, F. Li and H.-M. Cheng, *Advanced Materials*, 31 (2019) 3213.
7. L. Shao and S. Jin, *Journal of Cleaner Production*, 252 (2020) 113.
8. F. Duffner, N. Kronemeyer, J. Tübke, J. Leker and R. J. N. E. Schmuch, *Nature Energy*, 32 (2021) 213.
9. F. Schipper and D. Aurbach, *Russian Journal of Electrochemistry*, 52 (2016) 1095.
10. X. Hu, H. Jiang, F. Feng and B. Liu, *Applied Energy*, 257 (2020) 901.
11. X. Fang and H. Peng, *Small*, 11 (2015) 1488.
12. T. L. Kulova, V. N. Fateev, E. A. Seregina and A. S. Grigoriev, *International Journal of Electrochemical Science*, 15 (2020) 7242.
13. K. Han, T. Wang, N. Zhang, W. Zhang and T. J. E. A. Zhang, 365 (2021) 137232.
14. L. He, M. K. Hu, Y. J. Wei, B. J. Liu and Q. Shi, *Science China-Technological Sciences*, 63 (2020) 410.
15. S. Meisenzahl, P.-P. Sittig and M. Hoeck, *Chemie Ingenieur Technik*, 86 (2014) 1180.

16. S. Wang, C. Fernandez, X. Liu, J. Su and Y. Xie, *Measurement & Control*, 51 (2018) 125.
17. Y.-j. Ji, S.-l. Qiu and G. Li, *Journal of Central South University*, 27 (2020) 2606.
18. Y. Cai, Y. Che, H. Li, M. Jiang and P. Qin, *Journal of Power Electronics*, 21 (2021) 1530.
19. D. D. Chen, L. Xiao, W. D. Yan and Y. B. Guo, *Energy Reports*, 7 (2021) 320.
20. S. G. Stewart, V. Srinivasan and J. Newman, *Journal of the Electrochemical Society*, 155 (2008) A664.
21. S. Zhao, Z. Guo, K. Yan, S. Wan and G. J. E. S. M. Wang, *Energy Storage Materials*, 43 (2020) 901.
22. C. Jiang, S. Wang, B. Wu, C. Fernandez, X. Xiong and J. Coffie-Ken, *Energy*, 219 (2021) 545.
23. E. Kuzmina, E. Karaseva, A. Ivanov and V. Kolosnitsyn, *Energy Technology*, 7 (2019) 209.
24. L. Zhang, H. Peng, Z. Ning, Z. Mu and C. Sun, *Applied Sciences-Basel*, 7 (2017) 1081.
25. J. Xiao, Q. Li, Y. Bi, M. Cai, B. Dunn, T. Glossmann, J. Liu, T. Osaka, R. Sugiura, B. Wu, J. Yang, J.-G. Zhang and M. S. Whittingham, *Nature Energy*, 5 (2020) 561.
26. T. Ohzuku and R. J. Brodd, *Journal of Power Sources*, 174 (2007) 449.
27. X. Lai, Y. Zheng and T. Sun, *Electrochimica Acta*, 259 (2018) 566.
28. X. Bian, Z. Wei, J. He, F. Yan and L. Liu, *Ieee Transactions on Industrial Electronics*, 68 (2021) 12173.
29. X. Lai, S. Wang, S. Ma, J. Xie and Y. Zheng, *Electrochimica Acta*, 330 (2020).
30. Q. Wang, Z. Wang, L. Zhang, P. Liu and Z. Zhang, *Ieee Transactions on Transportation Electrification*, 7 (2021) 437.
31. Z. Wei, D. Zhao, H. He, W. Cao and G. Dong, *Applied Energy*, 268 (2020) 742.
32. R. Xiong, Q. Yu, L. Y. Wang and C. Lin, Applied Energy, 207 (2017) 346.
33. Y. Fan, H. Shi, S. Wang, C. Fernandez, W. Cao and J. J. E. Huang, *Energies*, 14 (2021) 2011.
34. S. Peng, X. Zhu, Y. Xing, H. Shi, X. Cai and M. J. J. o. P. S. Pecht, *Journal of Power Sources*, 392 (2018) 48.
35. S. H. Wang, Y. Yang and K. H. Guo, *Mathematical Problems in Engineering*, 2020 (2020) 672.
36. C. F. Yang, X. Y. Wang, Q. H. Fang, H. F. Dai, Y. Q. Cao and X. Z. Wei, *Journal of Energy Storage*, 29 (2020) 8711.
37. S. Wang and C. Jiang, *Energy*, 219 (2021) 119603.
38. X. Bian, Z. Wei, J. He, F. Yan and L. Liu, *Ieee Transactions on Transportation Electrification*, 7 (2021) 399.
39. P. Shen, M. Ouyang, L. Lu, J. Li and X. Feng, *Ieee Transactions on Vehicular Technology*, 67 (2018) 92.
40. F. Zheng, Y. Xing, J. Jiang, B. Sun, J. Kim and M. Pecht, *Applied Energy*, 183 (2016) 513.